Materials Letters 65 (2011) 289–292

Contents lists available at ScienceDirect

Materials Letters

journal homepage: www.elsevier.com/locate/matlet

End-closed NiCoFe-B nanotube arrays by electroless method

A. Azizi [a,b,*], M. Mohammadi [a,c], S.K. Sadrnezhaad [a,c]

[a] Department of Nanotechnology and Advanced Materials, Materials and Energy Research Center, P.O. Box 14155-4777, Tehran, Iran
[b] Department of Chemical and Biomolecular Engineering, Tulane University, New Orleans, LA 70118, USA
[c] Department of Materials Science and Engineering, Sharif University of Technology, P.O. Box 11155-9466, Tehran, Iran

ARTICLE INFO

Article history:
Received 17 September 2010
Accepted 5 October 2010
Available online 12 October 2010

Keywords:
End-close nanotube
Electroless
NiCoFe
AAO template
Metals and alloys
Nanocrystalline materials

ABSTRACT

A novel approach is obtained during the fabrication of NiCoFe-B nanotube arrays via electroless method. Porous anodic aluminum oxide (AAO) templates fabricated by anodization of aluminum foil were sensitized using $PdCl_2$ solution and immersed into electroless plating baths at room temperature to produce nanotube arrays. Compositional and morphological properties of the nanotube arrays are characterized. Results indicates the formation of end-closed nanotubes with the dimension of 100–130 nm in outside diameter, which is determined by the pore size of the AAO template, and about 15 nm in thickness of tube walls. The possible formation mechanism of end-closed metallic nanotube arrays is discussed.

1. Introduction

Self-assembling magnetic nanostructures have recently attracted much attention due to their potential applications [1,2]. Scientifically interesting properties of magnetic metal nanotubes have aggravated their use in nanomedicine, high-density magnetic recording media and sensing devices [2]. As a recent finding, nanotube arrays that are closed on one end have ability to utilize for drug delivery applications [3].

Using a porous template helps quick, inexpensive and environmentally benign preparation of nanotubes [4,5]. Various templates like track-etched membrane, diblock copolymer, polycarbonate and anodic aluminum oxide (AAO) have been used for structure formation. Among all these, the AAO has specific utilizations provoked by parallel pore channels and the holes that can be controlled by proper adjustment of the anodization conditions [6].

Both metallic nanotubes and nanowires can be assembled by chemical vapor deposition [7], electroplating [8] and supercritical fluids [9] on appropriately selected templates. Using electroless technique simplifies synthesizing method and the instrument that is required [10,11]. Electroless technique is a chemical deposition process which involves the use of chemical agents to coat an alloy onto the suitable sites of a template [4,12,13]. It does not need the electrical conductivity of the deposited substance and the deposition starts from pore walls and growth inwardly. Hollow fibrils or nanotubules have previously been produced, therefore, by this process [4].

This paper demonstrates the formation of NiCoFe nanotubes by electroless deposition method on AAO templates. What makes this work different from previous efforts is the formation of end-closed nanotubes which are announced for the first time by the specified method in this paper.

2. Material and methods

AAO templates were prepared by two-step anodization of annealed aluminum foil (99.99%-Merck). The foil was chemically treated in 1 M NaOH for 3 min at room temperature and rinsed with distilled water and acetone. The surface of the foil was eloctropolished in a mixture of $HClO_4$ and ethanol (1:4 in vol.) below 5 °C by applying 20 V voltage. Anodization was conducted for 20 h in 0.3 M phosphoric acid electrolyte under constant potential (120 V). A cooling system was used to keep the temperature unchanging (1.5 ± 1.5 °C). After the first anodization step, the porous film formed was stripped by immersion of the foil into a solution containing 2 wt.% phosphoric acid plus 6 wt.% chromic acid at 60 °C. Second anodization step was carried out with the same conditions were used in the first step. A rather uniform array of AAO nanowells were formed in this step.

Template pretreatment before the fabrication of NiCoFe nanotube arrays consisted of AAO immersion into an aqueous solution containing 1 g/L $PdCl_2$ and 12 g/L HCl kept under low vacuum situation for 3 min to enhance the solution into the pores. The procedure followed by polishing of the top surface with refined sandpaper. This is due to prevention of forming an unwanted alloy film on the AAO surface which seals the entrance of the pores preventing the nanotubes to

* Corresponding author. Department of Nanotechnology and Advanced Materials, Materials and Energy Research Center, P.O. Box 14155-4777, Tehran, Iran. Tel.: +98 9125322039; fax: +98 2166005717.
E-mail addresses: azizi@alum.sharif.edu, aazizi@tulane.edu (A. Azizi).

0167-577X/$ – see front matter © 2010 Elsevier B.V. All rights reserved.
doi:10.1016/j.matlet.2010.10.020

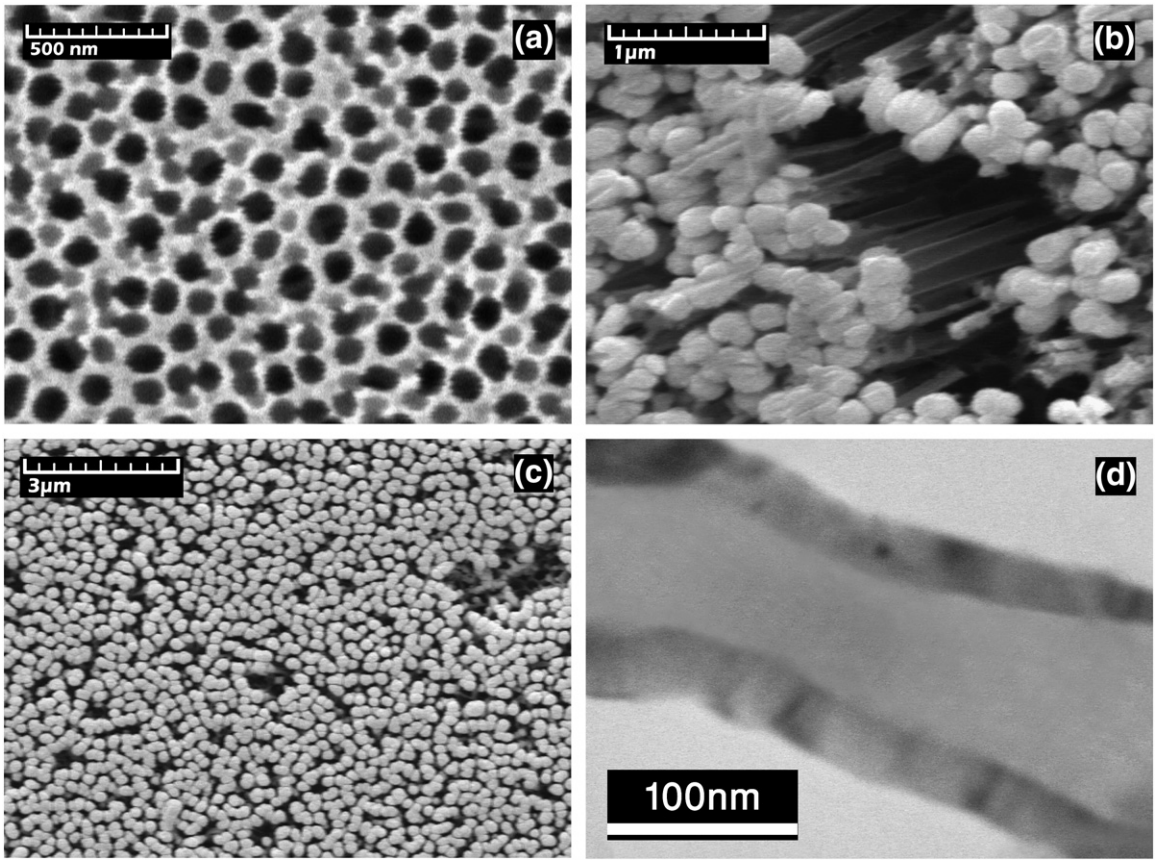

Fig. 1. (a) FE-SEM morphology of the anodized AAO and (b) side view FE-SEM, (c) top view FE-SEM and (d) TEM image of the end-closed NiCoFe-B nanotube arrays.

form [14]. The treated template was washed with deionized water and dried.

The formation of NiCoFe nanotube arrays was carried out by immersion of the treated AAO template into the electrolyte bath for 20 min at the room temperature. The bath contained 8.5×10^{-3} M $NiSO_4{\cdot}6H_2O$, 2.5×10^{-2} M $CoSO_4{\cdot}7H_2O$, 1.3×10^{-2} M $FeSO_4{\cdot}7H_2O$, 0.143 M lactic acid and 7×10^{-2} M DMAB and its pH was fixed at ~7–8. The selected pH was due to the fact that solutions with both higher and lower pH values could corrode the AAO membrane.

Morphologies of both the AAO and the metallic nanotubes were characterized and compared. Field emission scanning electron microscope (FE-SEM) and transmission electron microscope (TEM) were used for this purpose. In order to obtain a better morphology for the NiCoFe, partial dissolution of the AAO membrane into 1 M NaOH was of help. Energy dispersive X-ray spectrometer (EDS) and inductively coupled plasma-optical emission spectrometer (ICP-OES) were also employed to determine the chemical composition of the nanotubes.

3. Results and discussion

Fig. 1(a) illustrates the morphology of the AAO template. Its diameter pores is estimated about 100–120 nm.

Fig. 1(b) shows the FE-SEM image of the 20 min coated AAO template. As is seen in the figure, 20 min deposition results in nanotube NiCoFe-B array creation. An interesting phenomenon is end-closed nanotube formation. To the best of the authors' knowledge, this is the first time that the end-closed NiCoFe-B nanotube arrays are formed during electroless deposition procedure. Fig. 1(c) illustrates the top view of the synthesized nanotubes indicating good order, separation and uniformity of the produced nanotube arrays.

The TEM image of the NiCoFe-B nanotubes fabricated by explained procedure is seen in Fig. 1(d). Image analysis of the nanotubes microstructure indicated about 110 nm for their outer diameter, corresponding well to the average internal diameter of the pores on the AAO. According to the TEM image, average wall thickness of the nanotubes is about 15 nm. These figures are related to the electroless deposition conditions and can simply be controlled by template fabrication parameters [5].

The reactions ending in NiCoFe-B nanotube arrays formation are as follows [6,15]:

$$Pd^{2+}+2e=Pd \quad E^0=915\,mV \tag{1}$$

$$Ni^{2+}+2e=Ni \quad E^0=-250\,mV \tag{2}$$

$$Co^{2+}+2e=Co \quad E^0=-280\,mV \tag{3}$$

$$Fe^{2+}+2e=Fe \quad E^0=-440\,mV \tag{4}$$

The standard electrode potentials of the reduction reactions are shown by E^0. In the electroless deposition process, the electrode potential of the oxidation reactions for reduced agent is lower than the reduction potential of the metallic ions present in the bath [15]. At larger metal electrode potentials, the difference between the oxidizer and the reductant potentials will become greater. This leads to a higher possibility for the redox reaction [6].

Reduction of metal and oxidation of boron ions by DMAB can be described by the following reactions [15]:

$$3Me^{2+}+2R_2NHBH_3+6H_2O=3Me^0+2R_2NH_2^++2B(OH)_3+3H_2+4H^+ \tag{5}$$

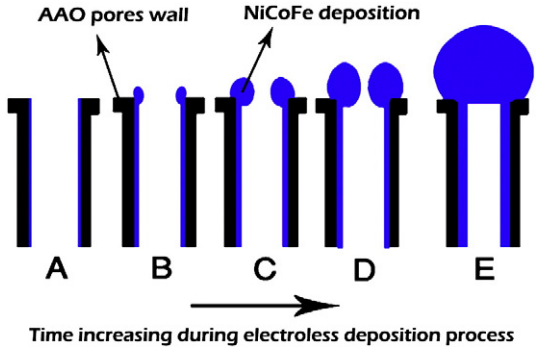

Fig. 2. The schematic diagram representing the stages of end-closed nanotube formation during the electroless deposition process.

$$R_2NHBH_3 \xrightarrow{Catalyst} R_2NH + BH_3 + H_2 + H^+ \rightarrow R_2NH_2^+ + B + 5/2H_2 \quad (6)$$

Eqs. (5) and (6) can be combined as follows:

$$3Me^{2+} + 3R_2NHBH_3 + 6H_2O = 3Me^0 + B + 3R_2NH_2^+ + 2B(OH)_3 + 9/2H_2 + 3H^+ \quad (7)$$

in which Me represents Pd, Ni, Co or Fe and R shows the (CH_3) group. This mechanism explains production of gaseous hydrogen together with the pH decrease and H^+ release during the nanotube formation within the bath.

Based on the reduction potential of the metal ions given in Eqs. (1)–(4), Pd^{2+} reduction by DMAB is easier than Ni, Co and Fe. The reduced Pd nanoparticles are deposited on the surface of the pore walls of the AAO template. Reduction of Ni, Co and Fe occurs subsequently via the catalytic effect of Pd.

The total reaction (7) of the electroless deposition process can be used to explain the possible mechanism by which the end-closed nanotubes are formed. It has been mentioned earlier that the pH of the coating bath decreases by the deposition reactions [15]. Since the solution is not agitated, the pH in locations next to the deposition surfaces sharply changes. The limited amount of the coating solution inside the pores results in more significant pH reduction within the pores. The deposition rate at these locations is hence very low. The pH of the solution outside the AAO pores is, on the other hand, more. The result is higher deposition rates near the end of the nanotube holes as compared to the inside of the pores. This leads to accumulation of spherical clusters at nanotube ends which cause their ends become closed. The stages involved in NiCoFe end-closed nanotube formation are schematically depicted in Fig. 2.

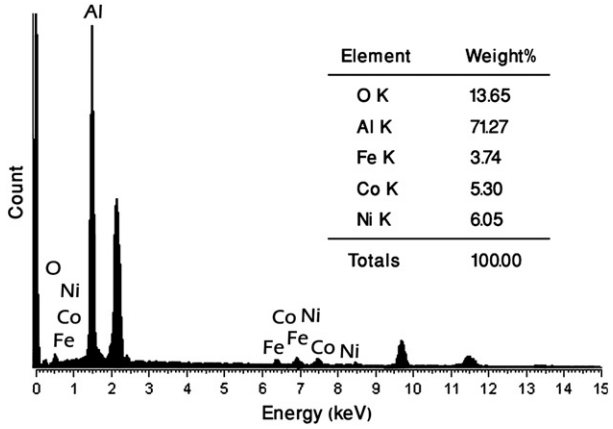

Fig. 3. EDX spectrum of the AAO template containing NiCoFe nanotubes.

Table 1
Mole percent of the elements in the plating bath and on the AAO.

Element	Nickel	Cobalt	Iron
Mol percent in the plating bath	20	52	28
Mol percent in the coating	40	35	25

It seems attractive here that the end-closed nanotube formation does not interrupt during the electroless deposition process, despite the fact that the gaseous hydrogen evolves out of the deposition surface. It may be concluded that the closed ends of the nanotubes have foamy-like morphology. The probable mechanism is the formation of new atom simultaneously with the exit of the gaseous hydrogen from the pores wall of the AAO at the final stages of the process. It may result in the formation of the NiCoFe clusters with mesoporous-like morphology on the top of the tubes.

The EDX analysis of the nanotubes fabricated on the surface of the AAO template is shown in Fig. 3. The figure shows the presence of nickel, cobalt and iron in the AAO indicating the nanotubes arrays being NiCoFe alloy. The O and Al peaks belong to the substrate AAO. The boron content of the coatings, which is taken in plated film from reducing agent of dimethylamine borane (DMAB) cannot be detected by EDX analysis [16]. Table 1 compares the mole percentages of the metals in the coating and in the plating bath. The data indicates that the molar content of the elements in the nanotubes are not the same as those in the plating bath. Nickel content is, for example, larger of the coating than cobalt and iron; while its concentration is the lowest in the coating bath. The reduction potential of the nickel ions is lower than those for cobalt and iron [6,15]. This seems responsible for greater nickel content in the nanotubes deposited on the AAO. The ICP result also showed that the boron content of the nanotubes is ~0.67 at.%.

4. Conclusions

End-closed NiCoFe-B nanotubes are deposited on prepolished anodized aluminum foil via electroless method. A mechanism is devised to explain the pH related deposition of the nanotube structures formed with close ends. Surface characterization and analysis of the nanotube arrays indicate the significance of the geometry of the AAO holes and the reduction potential of the depositing elements from the coating solution.

References

[1] Elías AL, Rodríguez-Manzo JA, McCartney MR, Golberg D, Zamudio A, Baltazar SE, et al. Production and characterization of single-crystal FeCo nanowires inside carbon nanotubes. Nano Lett 2005;5(3):467–72.
[2] Li FS, Zhou D, Wang T, Wang Y, Song LJ, Xu CT. Fabrication and magnetic properties of FeCo alloy nanotube array. J Appl Phys 2007;101 014309-014309-3.
[3] Gasparac R, Kohliv P, Mota MO, Trofin L, Martin CR. Template synthesis of nano test tubes. Nano Lett 2004;4(3):513–6.
[4] Cao G, Liu D. Template-based synthesis of nanorod, nanowire, and nanotube arrays. Adv Colloid Interface Sci 2008;136:45–64.
[5] Wang W, Li N, Li X, Geng W, Qiu S. Synthesis of metallic nanotube arrays in porous anodic aluminum oxide template through electroless deposition. Mater Res Bull 2006;41:1417–23.
[6] Ren X, Jiang CH, Huang XM, Li DD. Fabrication and magnetic behavior of chemical deposited Ni–P nanowire and nanotube arrays. Physica E 2009;41:349–52.
[7] Li MK, Lu M, Kong LB, Guo XY, Li HL. The synthesis of MWNTs/SWNTs multiple phase nanowire arrays in porous anodic aluminum oxide templates. Mater Sci Eng A 2003;354:92–6.
[8] Fu J, Cherevko S, Chung CH. Electroplating of metal nanotubes and nanowires in a high aspect-ratio nanotemplat. Electrochem Commun 2008;10(4):514–8.

[9] Xu J, Zhang W, Morris MA, Holmes JD. The formation of ordered bismuth nanowire arrays within mesoporous silica templates. Mater Chem Phys 2007;104:50–5.
[10] Rohan JF, Casey DP, Ahern BM, Rhen FMF, Roy S, Fleming D, et al. Coaxial metal and magnetic alloy nanotubes in polycarbonate templates by electroless deposition. Electrochem Commun 2008;10:1419–22.
[11] Mohammadi M, Ghorbani M, Azizi A. Effect of specimen orientation and heat treatment on electroless Ni-PTFE-MoS2 composite coatings. J Coat Technol Res in press.
[12] Hou S, Harrell CC, Trofin L, Kohli P, Martin CR. Layer-by-layer nanotube template synthesis. J Am Chem Soc 2004;126(18):5674–5.
[13] Xie G, Wang Z, Li G, Shi Y, Cui Z, Zhang Z. Templated synthesis of metal nanotubes via electroless deposition. Mater Lett 2007;61:2641–3.
[14] Li N, Li X, Yin X, Wang W, Qiu S. Electroless deposition of open-end Cu nanotube arrays. Solid State Commun 2004;132:841–4.
[15] Mallory GO. The fundamental aspects of electroless nickel plating. In: Mallory GO, Hajdu JB, editors. Electroless Plating: Fundamentals and Applications. Florida: AESF Society; 1990. p. 1–56.
[16] Zhu X, Dong H, Lu K. Coating different thickness nickel–boron nanolayers onto boron carbide particles. Surf Coat Technol 2008;202:2927–34.